KFUPM
Journal of Undergraduate Research International

Diamond Open Access 143

Article Mechanical Engineering

Passive Thermal Management of Satellite Photovoltaic Panels Using Phase Change Materials

Ahmad Aloufi and Naef A. A. Qasem*

Cite https://doi.org/10.64589/juri/231568

Submitted: April 23, 2026 Revised: May 11, 2026 Accepted: May 13, 2026

ABSTRACT

This study investigated the thermal behavior of photovoltaic (PV) panels in low Earth orbit (LEO) and evaluated the use of phase-change materials (PCMs) for passive thermal control. In space, PV panels experience large temperature fluctuations during orbital cycling, which can reduce their efficiency and affect system reliability. In this work, a numerical model was developed using COMSOL Multiphysics software to simulate the transient thermal behavior of a multilayer PV panel under space conditions, including solar radiation, radiation to deep space, and the PCM phase change process. Various PCM materials, namely n-hexadecane, n-heptadecane, and n-octadecane, were investigated together with different aluminum fin thicknesses and PCM heights to determine the optimal configuration. The results showed that in the absence of a PCM, the PV panel reached a peak temperature of ~71 °C, while PCM integration minimized temperature fluctuation. Among the tested materials, n-hexadecane exhibited the optimal performance, reducing the peak temperature to nearly 22 °C, corresponding to an improvement of ~69%. Additionally, a PCM height of 20 mm provided the optimal thermal performance, while an aluminum thickness of 4 mm achieved superior balance between heat conduction and thermal storage, resulting in improved thermal regulation and higher PV efficiency. Overall, the combination of the PCM and the optimized aluminum design was found to be effective in the passive thermal management of PV panels under space conditions.

Keywords: space photovoltaic panels, low Earth orbit (LEO), passive thermal management, phase change material (PCM)

1. INTRODUCTION

Over 10,000 active satellites exist in low Earth orbit (LEO), driven by large-scale constellations[1]. Currently, photovoltaic (PV) panels constitute the main power sources for LEO satellites, with rechargeable batteries being employed during eclipses[2]. One of the main challenges associated with the use of PV panels in LEO is the large temperature swing during each orbital cycle. Previous studies have shown that spacecraft solar-array temperatures can decrease to approximately −33 °C (240 K) during eclipse and increase to nearly 107 °C (380 K) under direct solar radiation[3], as shown in Figure S1 in the Supplementary Information. This significant thermal cycling can affect both PV performance and structural reliability. Since the focus of the present study is thermal regulation under LEO conditions, the subsequent discussion emphasizes the thermal behavior of PV panels in LEO.

A typical PV module converts ~6–20% of incident sunlight into electricity, depending on the cell type and local environmental conditions[3]. Studies have shown that an ~1 °C increase in solar cell temperature can reduce its efficiency by nearly 0.45%[4]. Given the substantial temperature fluctuations encountered in space, addressing this effect is essential to ensure the reliable performance of the satellite power subsystem.

Several passive thermal control methods are commonly used in spacecraft to regulate temperature under space conditions. For instance, thermal control coatings are applied to manage the balance between absorbed solar radiation and emitted heat, allowing surfaces to maintain acceptable temperature levels. However, the coating performance degrades over time due to exposure to atomic oxygen, ultraviolet radiation, and thermal cycling, leading to increased solar absorptance and reduced effectiveness[5]. Multilayer insulation (MLI), based on multiple reflective layers separated by spacers, is also commonly employed to minimize radiative heat transfer. Although MLI effectively reduces heat exchange, it cannot be applied to the front surface of a PV panel as it blocks solar radiation. Additionally, when applied to the rear of the PV, it primarily acts as a thermal barrier, but does not prevent a rise in temperature upon sunlight exposure[6]. Radiators are also employed to dissipate excess heat by emitting thermal radiation into deep space. Although radiators effectively remove internally generated heat, their performance depends on their orientation and exposure to deep space, and they are less effective at mitigating the rapid temperature fluctuations experienced during orbital cycles[7]. These limitations highlight the requirement for alternative thermal management approaches capable of regulating temperature and reducing thermal fluctuations.

Published under an exclusive license by KFUPM

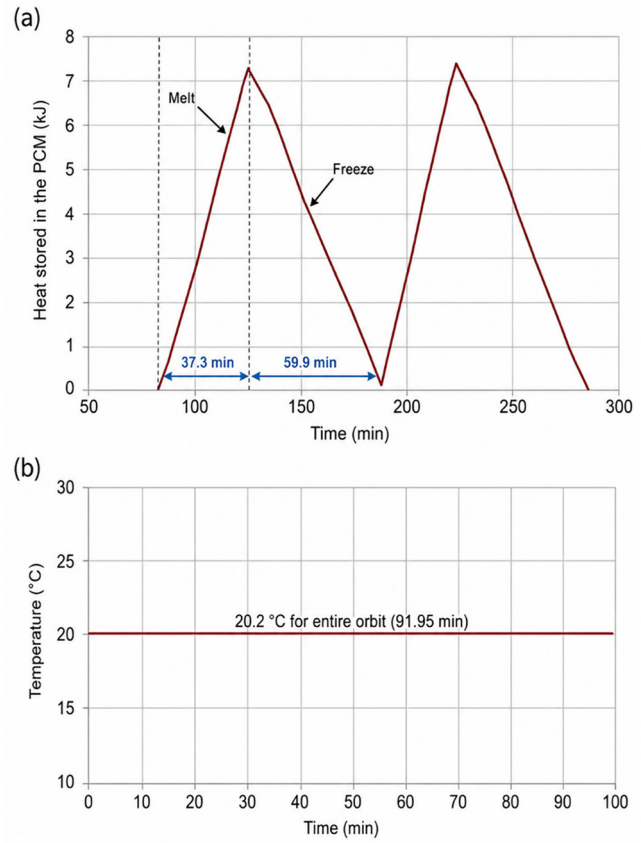


Figure 1. PCM thermal behavior over an orbital cycle: (a) Melt–freeze cycling and (b) managed temperature over a complete orbit [8]

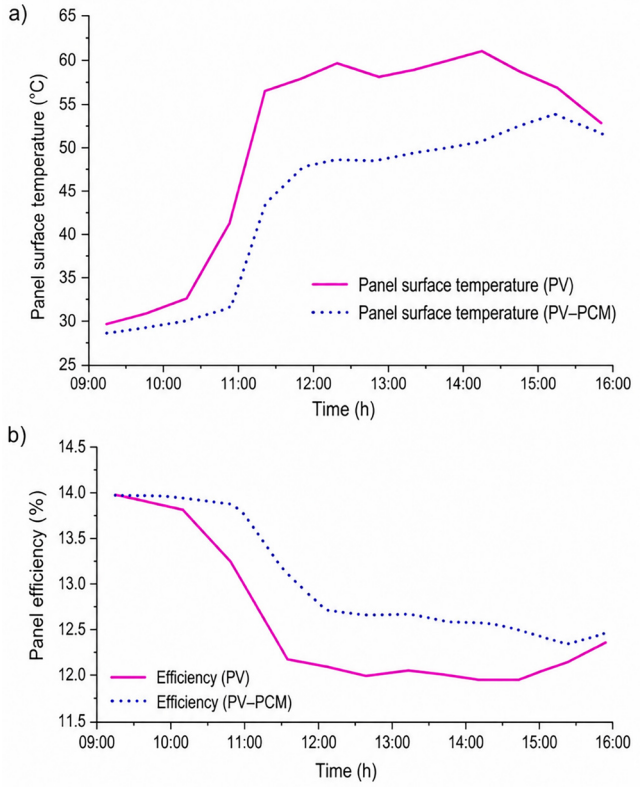


Figure 2. Experimental comparison between conventional PV and PV–PCM systems under terrestrial conditions. Variation in the (a) PV surface temperature and (b) PV efficiency over time [9]

Consequently, phase-change materials (PCMs) have emerged as a promising passive thermal management solution. PCMs absorb and release large amounts of heat during phase transitions, allowing them to regulate the temperature and reduce thermal fluctuations without requiring external power. In the context of space applications, NASA investigated the use of n-hexadecane as a PCM for the thermal regulation of the IceCube CubeSat electronics system under International Space Station-like orbital conditions [8]. This PCM was used to maintain the temperature of the mixer/local-oscillator assembly and the intermediate-frequency assembly close to 20 °C (±1 °C) during orbital thermal cycling. Notably, n-hexadecane has a melting temperature of ~18.2 °C, which allows it to melt during sunlight exposure and solidify during eclipse periods over an ~92 min orbit. As illustrated in Figure 1(a) and Figure 1(b) [8], the PCM undergoes continuous melt–freeze cycling during sunlight and eclipse periods, where heat is absorbed during melting and released during solidification. It was revealed that the temperature of the electronic components remained close to 20 °C for almost a complete orbit, thereby demonstrating the potential of PCMs for passive thermal regulation in space.

Similarly, in terrestrial PV systems, PCMs have been shown to significantly reduce the operating temperature and enhance PV performance. One experimental study investigated two similar PV panels, namely one equipped with a PCM cooling system based on calcium chloride hexahydrate (melting temperature ~29 °C) and one without a PCM [9]. The PCM was enclosed within an aluminum container bearing Al fins and attached to the rear surface of the PV panel (tilt angle = 30°) to promote heat transfer.

As illustrated in Figure 2(b), the PV-PCM system achieved a ~6.85% improvement in operational efficiency, indicating in operational efficiency, indicating a clear reduction in overheating and improved power generation capability. These results demonstrate that the PCM effectively reduces the PV operating temperature and enhances thermal regulation.

Recently, Liu and Li [10] investigated PCM-based thermal management for fixed solar panels in nanosatellites operating in LEO using electro–thermal coupling analysis to account for the relationship between temperature variation and electrical performance. Rubitherm RT57HC, a commercial paraffin-based PCM with a main melting peak of approximately 57 °C, was selected owing to its suitable melting-temperature range for orbital thermal regulation. It was revealed that PCM integration significantly reduced the solar panel temperature fluctuation from 7.187 to 0.826 K, corresponding to a reduction of ~88.5%. Additionally, the selection of an appropriate PCM melting temperature improved the steady-state thermal behavior of the solar panels during orbital operation, demonstrating the potential of PCM-based passive thermal management for improving thermal stability and maintaining reliable PV performance under orbital thermal cycling conditions.

Most previous studies on PCM thermal management have focused either on terrestrial PV systems [10] or on the thermal regulation of spacecraft electronic components [9]. More recently, PCM integration was investigated for nanosatellite PV panels operating in LEO [11]. Although these studies demonstrated

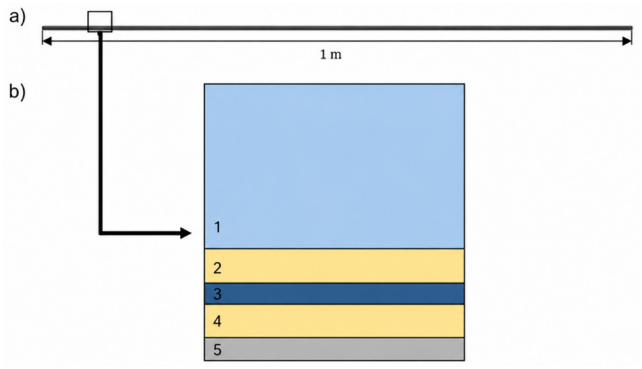


Figure 3. Modeled geometry of the multilayer PV panel: (a) Panel geometry with a width of 1 m, and (b) detailed view of the layered structure across the panel thickness. (1) Glass, (2, 4) EVA, (3), Si, and (5) the back sheet

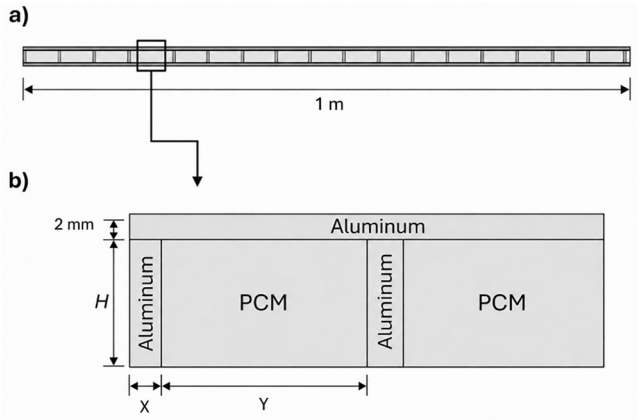


Figure 4. Configuration of the PCM–Al thermal management system: (a) Overall view aligned with the 1 m PV panel width, and (b) detailed view showing the PCM regions enclosed within an Al container with internal fins. The geometric parameters are also shown

the capability of PCMs to reduce temperature fluctuations and improve thermal stability, further investigation is required regarding the combined effects of material and structural factors on the thermal performance of space PV panels under orbital thermal cycling conditions.

The aim of the current study is therefore to develop a transient numerical model for a multilayer PV panel integrated with a PCM under space conditions, while investigating the effects of different PCM materials, PCM heights, and Al fin thicknesses on the thermal regulation of PV panels during orbital operation.

2. METHODOLOGY

2.1. Physical Model. A standard multilayer PV panel was modeled to represent the baseline system. The panel consisted of five layers: glass, ethylene-vinyl acetate (EVA), silicon (Si), EVA, and a backsheet, arranged sequentially from the top surface, as shown in Figure 3. The thickness and thermal properties of each layer were defined based on typical PV module configurations, and the detailed values are provided in Table S1 in the Supplementary Information[12]. The layers were assumed to be perfectly bonded, allowing one-dimensional heat transfer through the panel thickness.

The configuration of the PCM–Al thermal management system used in this study is illustrated in Figure 4. Three types of PCM were considered in this study, and their thermal properties were defined based on values reported in the literature[13]. The detailed thermal properties of the selected PCMs are provided in Table S2 in the Supplementary Information. Notably, one of the main limitations associated with PCMs is their relatively low thermal conductivity, which reduces their heat-transfer rate. To address this issue, an Al container and fins were employed to enhance heat conduction. The thermal properties of Al were taken as standard values, with a density of 2700 kg/m^3, thermal conductivity of 220 W/m · K, and specific heat capacity of 900 J/kg · K. Additionally, different Al thicknesses (X) were investigated, namely 2, 4, and 6 mm. To maintain a constant number of PCM compartments, namely 20 packs, the corresponding PCM widths (Y) were adjusted to 48, 46, and 44 mm, respectively. Moreover, the height (H) of the PCM was set at 20, 17, or 15 mm.

2.2. Governing Equations. The thermal behavior of the PV–PCM system was modeled using transient heat transfer equations, including heat conduction, radiative heat exchange, and the PCM phase-change process. The temperature distributions in the PV panel, Al structure, and PCM are governed by the heat conduction equation presented in Eq. (1)[11]:

$$\rho c_p \frac{\partial T}{\partial t} = \nabla \cdot (k \nabla T) + Q \tag{1}$$

where ρ is the density (kg/m^3), $c_p$is the specific heat capacity (J/kg · K), T is the temperature (K), k is the thermal conductivity (W/m · K), and Q represents the volumetric heat generation term (W/m^3), which occurs primarily in the PV layer as a result of solar radiation absorbed by the material. Since the investigated system operates in space, heat loss from the surface is mainly due to thermal radiation. The radiative heat flux is given by Eq. 2[11]:

$$q = \varepsilon \sigma \left(T^4 - T_{sky}^4 \right) \tag{2}$$

where q is the radiative heat flux (W/m^2), ε is the surface emissivity, σ is the Stefan–Boltzmann constant (5.67×10^{-8} W/(m^2·K^4)), and T_{sky} is the deep-space temperature (K). The phase-change process was modeled using the enthalpy method, which accounts for both sensible and latent heat during melting and solidification. The governing equation is given by Eq. 3[11]:

$$\rho \frac{\partial h}{\partial t} = \nabla \cdot (k \nabla T) + Q \tag{3}$$

where h is the specific enthalpy (J/kg), ρ is the density (kg/m^3), T is the temperature (K), k is the thermal conductivity (W/m · K), and Q is the volumetric heat generation term (W/m^3). In the PCM region, h incorporates both sensible and latent heat during the phase-change process. If no internal heat generation is applied within the PCM, Q is considered to be zero in the PCM domain. The PV efficiency was calculated as a function of the Si layer temperature using a temperature-dependent relationship, as detailed in Eq. 4[12]:

$$\eta = \eta_{\text{ref}} \left[1 - \beta \left(T_{\text{cell}} - T_{\text{ref}} \right) \right] \tag{4}$$

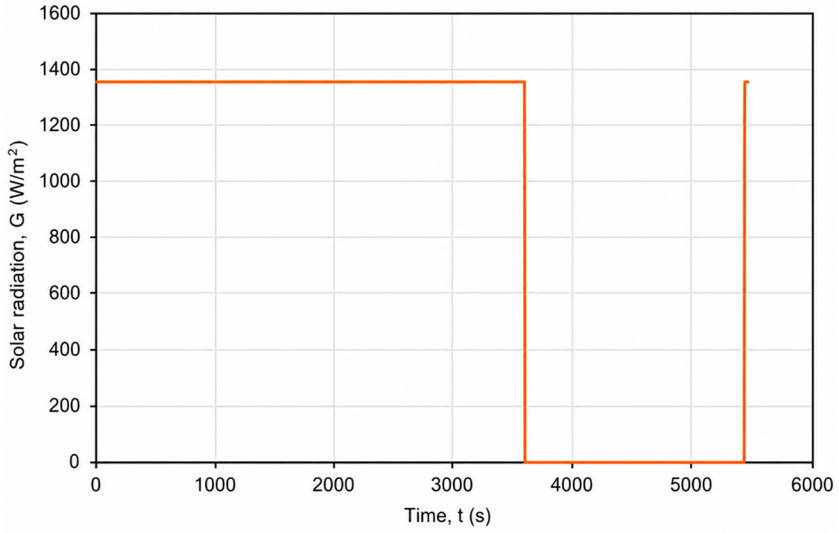


Figure 5. Time-dependent solar radiation $G(t)$ during one orbital cycle

where η is the PV efficiency, η_{ref} is the reference efficiency at the reference temperature T_{ref} (i.e., 0.20 at 20 °C), β is the temperature coefficient (0.004 1/K), and T_{cell} is the Si layer temperature. This relationship shows that efficiency decreases linearly with increasing temperature, thereby highlighting the importance of thermal regulation in improving PV panel performance. The above equations were solved using COMSOL Multiphysics software[11] under transient conditions.

2.3. Boundary Conditions. Figure 5 shows the variation in solar radiation $G(t)$ with time during one orbital cycle. In the sunlit region, solar radiation was assumed to be 1361 W/m^2, representing the solar radiation constant in LEO under space conditions[13]. During the eclipse period, the solar radiation was taken as zero. It was also assumed that the PV panel is always oriented toward the sun; therefore, solar radiation contacts the surface without any angular losses. Figure 6 shows the applied boundary conditions for the PV–PCM system. The top surface is exposed to time-dependent solar radiation $G(t)$, and heat is lost from the same surface through radiation to space. Solar radiation was assumed to be absorbed directly by the Si layer with an absorptivity of 0.90, whereas the front glass layer radiated heat to space with an emissivity of 0.9, based on typical values reported in the literature[14]. The bottom surface and sides were thermally insulated, and convective heat transfer was neglected since the system operates in a vacuum environment. Additionally, the effects of infrared radiation and the Earth's albedo were neglected to simplify the model and focus on the dominant heat transfer mechanisms. However, heat conduction still occurred within the system, particularly between the different layers of the PV panel and the PCM unit.

2.4. Numerical Model. A numerical model was developed using COMSOL Multiphysics software to simulate the thermal behavior of the integrated PV–PCM system over a period of 5400 s, which represents a typical LEO orbit. A mesh-independent study was conducted for the full PV–PCM model after integration. The liquid fraction of the PCM at $t = 1400$ s was selected as the reference parameter. Several mesh sizes with different numbers of elements were tested, and the results are presented in Figure 7. It can be observed that the liquid fraction increases slightly at lower mesh densities but becomes essentially constant as the number of elements increases. In particular, minimal differences were observed beyond the 134,777 elements, indicating that the solution was almost independent of further mesh refinement. Therefore, a mesh with 134,777 elements, as shown in Figure 8, was selected for the final simulations, as it provided stable results with lower computational time compared to finer meshes.

2.5. Model Validation. To verify the accuracy of the developed model, a validation study was performed on a PV panel in the absence of a PCM, and the results were compared with experimental data reported by Khyani et al.[15]. Figure 9 shows a comparison between the simulation and reference results, where the temperature of the back sheet layer is plotted over time. Overall, the two sets of results correlated well, with only small differences observed throughout the simulation period.

Figure 10 shows a comparison between the two sets of results, in which the liquid fraction of the PCM is plotted over time. The simulation followed the same trend as the experimental data with only small differences observed throughout the melting process.

3. RESULTS AND DISCUSSION

Figure 11 shows the variation in temperature for the Si layer both in the presence and absence of the PCM during one orbital period, together with the applied solar radiation $G(t)$. In the absence of the PCM, the temperature increased rapidly during the sunlight period, ultimately exceeding 70 °C due to the continuous absorption of solar radiation. After entering the eclipse region, the temperature dropped sharply through radiative heat loss into space. In contrast, upon PCM incorporation, a significantly reduced and more gradual temperature rise was observed, and the peak temperature remained at ~21.5 °C. This can be attributed to heat absorption by the PCM during the phase-change process. Additionally, the PCM system exhibited smaller temperature fluctuations and the drop during the eclipse period

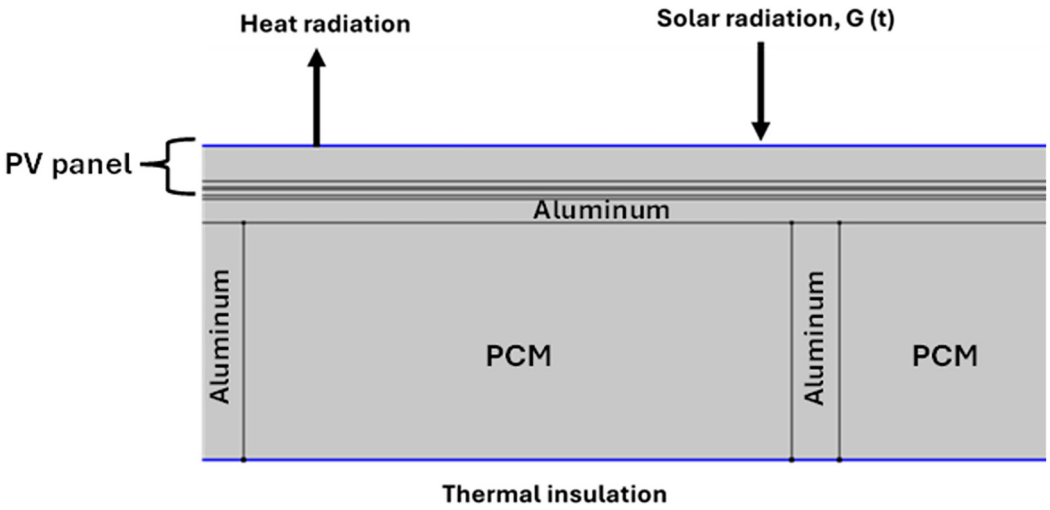


Figure 6. Boundary conditions applied to the PV–PCM system

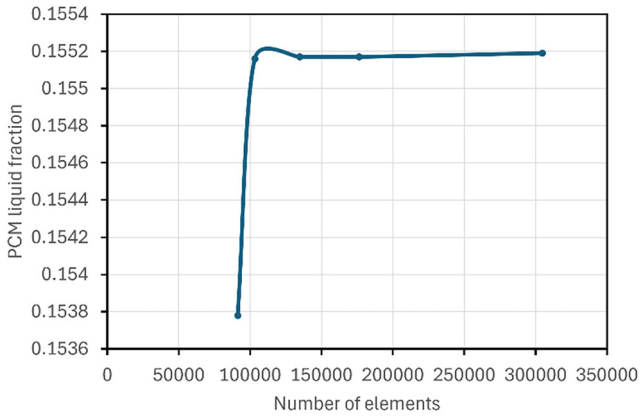


Figure 7. Mesh refinement for the PV–PCM system

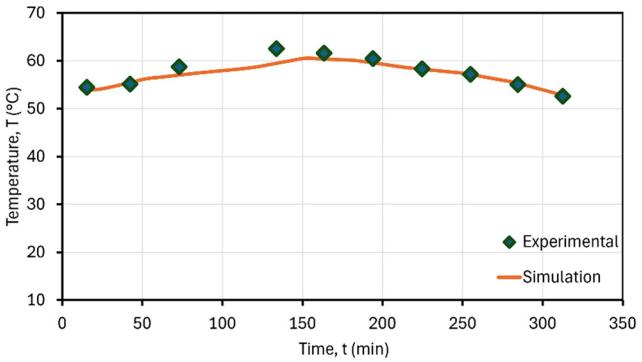


Figure 9. Validation of the PV panel model. Comparison between the present simulation and the experimental back sheet temperature [15]

was less pronounced. Notably, the simplified model may have influenced the outcome, and thus the actual results could differ slightly. Nevertheless, these findings indicate that the PCM effectively reduces temperature fluctuations and enhances the thermal stability of the PV panel.

Subsequently, the effects of three PCM types, namely n-hexadecane, n-heptadecane, and n-octadecane, on the thermal performance of the PV panel were investigated for a fixed Al thickness (X = 4 mm) and PCM height (H = 20 mm), as shown in Figure 12. The thermal properties of the corresponding PCMs are listed in Table S2 in the Supplementary Information. From Figure 12(a) it is evident that all PCMs reduced the PV temperature compared with the baseline case. However, clear differences can be observed between the three materials. Specifically, n-hexadecane yielded the lowest temperature during the majority of the orbital period, followed by n-heptadecane, whereas n-octadecane resulted in the highest temperature. This behavior was primarily due to the differences in melting temperature and thermal properties of the three PCMs. Materials with lower melting temperatures begin absorbing heat earlier, thereby reducing the peak temperature more effectively. The superior performance

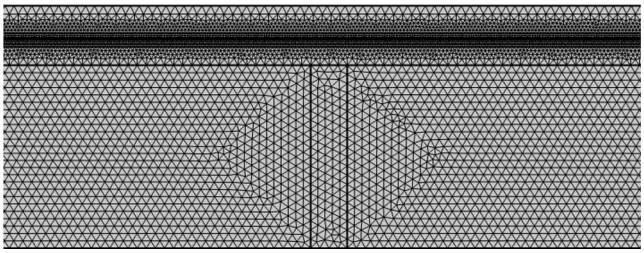


Figure 8. Final mesh configuration of the PV–PCM model used for the simulation following mesh refinement (134,777 elements)

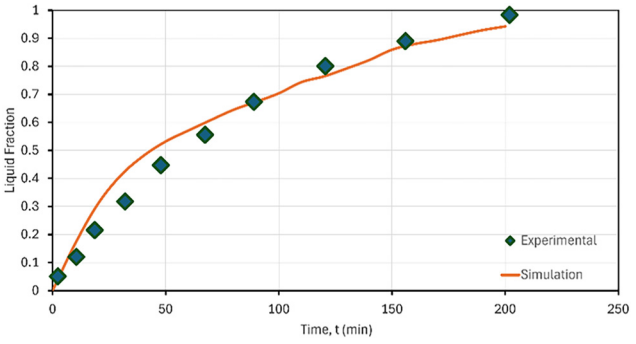


Figure 10. Validation of the PCM model. Comparison between the present simulation and the experimental liquid fraction [16]

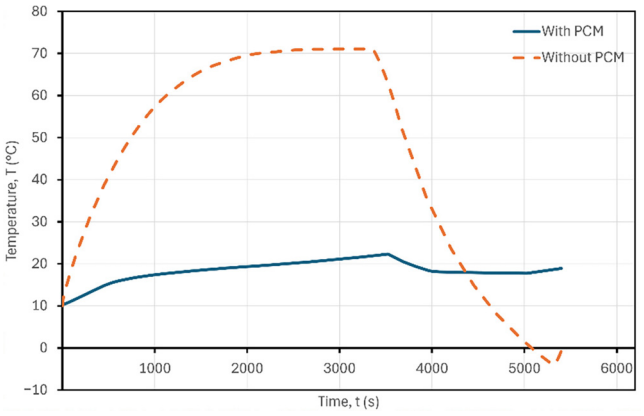


Figure 11. Comparison of Si layer temperature with and without the PCM under space conditions over one orbital period

of n-hexadecane was therefore attributed to its lower melting temperature, which enables earlier initiation of the phase change process during heating. Consequently, a larger portion of the absorbed thermal energy is stored as latent heat, leading to improved thermal regulation within the PV panel. This behavior was consistent with the findings of Choi et al.[8], who revealed that n-hexadecane demonstrated effective thermal stabilization owing to its suitable melting temperature under orbital thermal cycling conditions. In contrast, n-octadecane led to higher operating temperatures as its higher melting temperature delayed the activation of the phase-change process. Consequently, more heat is initially absorbed as sensible heat before latent heat absorption comes into play, resulting in a larger temperature increase. It should be noted that the solar radiation function and orbital sunlight duration were maintained constant for all simulated cases. The slight variation in the location of the temperature peak was caused by the thermal inertia and latent heat storage behavior of the PCM, which delayed the thermal response of the PV panel during the heating and cooling stages of the orbital cycle. The same trend can be observed in Figure 12(b) in which the PV efficiency is plotted over time. Specifically, n-hexadecane led to the highest PV efficiency, whereas n-octadecane resulted in the lowest efficiency. These results can be accounted for by considering that a lower operating temperature leads to superior PV performance. Consequently, n-hexadecane provided optimal thermal regulation and PV performance under the investigated conditions.

Subsequently, using n-hexadecane as the optimal PCM, the effect of PCM height on the PV–PCM system was investigated for a fixed Al thickness of 4 mm, as shown in Figure 13. From Figure 13(a), it is evident that a height of 20 mm yields the lowest temperature over the majority of the heating period, with taller and shorter PCMs resulting in higher temperatures. Although increasing the height to 25 mm led to a greater PCM volume, the cooling performance was not enhanced. A similar behavior was reported by Bria et al.[17], where thicker PCMs failed to achieve full melting during operation. This behavior was mainly attributed to the low thermal conductivity of the PCM, which limits heat penetration into deeper PCM regions during orbital heating. Consequently, the PCM layers located near the PV panel absorb most of the incoming thermal energy to undergo a phase change, whereas the deeper PCM regions remain partially unmelted and do not effectively participate in latent heat absorption. Consequently, in the current system, the additional PCM volume was not fully utilized, leading to a limited improvement in thermal regulation despite the increase in PCM height. This trend is also reflected in Figure 13(b), where a relatively higher efficiency is observed for a height of 20 mm, reflecting superior thermal control. Thus, H = 20 mm was considered the optimal configuration among the tested specimens.

Figure 14 shows the influence of different Al fin thicknesses (i.e., 2, 4, and 6 mm) on system performance. To maintain constant overall geometry, the corresponding PCM thicknesses were adjusted to 48, 46, and 44 mm, as discussed below. From Figure 14(a), it is evident that a fin thickness of 4 mm yields the lowest temperature for the Si layer throughout the majority of the orbital period. Slightly higher temperatures were observed for 2 mm thickness, while an increased thickness of 6 mm resulted in the highest temperature. This suggests that increasing Al fin thickness does not always lead to improved thermal performance. Thus, although a thicker fin can enhance heat conduction, it also reduces the available PCM thickness, which lowers the heat stor-

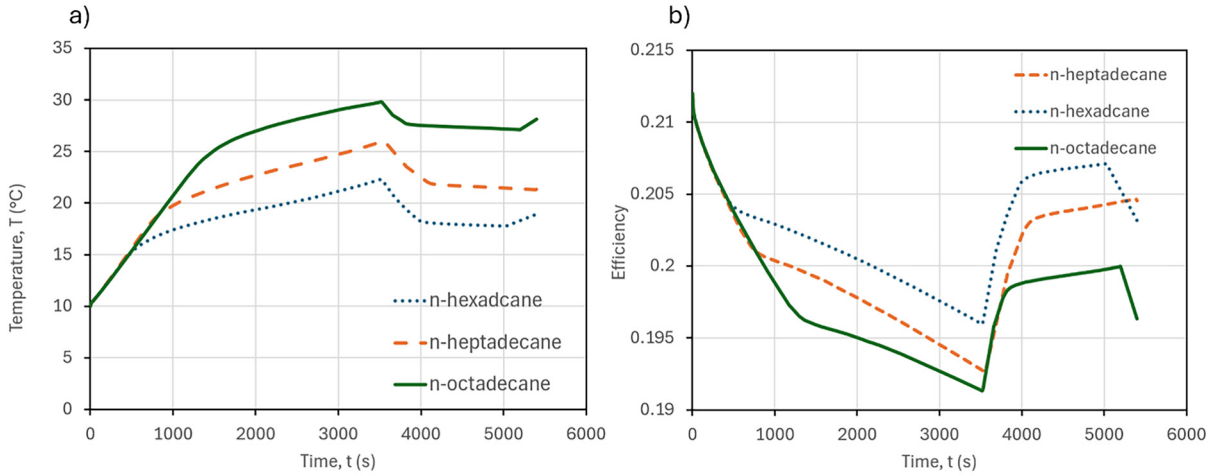


Figure 12. Effect of PCM type on PV performance under space conditions: (a) Si layer temperature and (b) PV efficiency

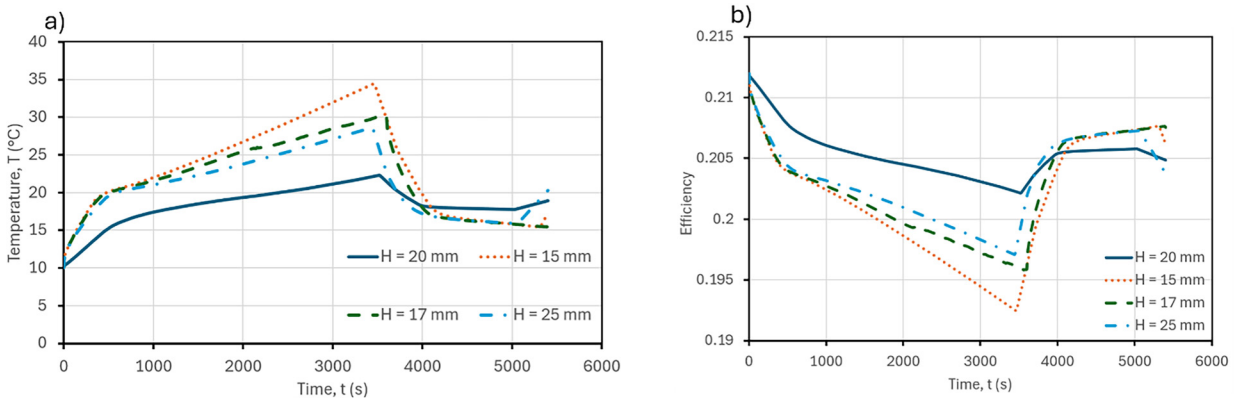


Figure 13. Effect of PCM height (H) on system performance: (a) Variation in the Si layer temperature with time, and (b) corresponding PV efficiency for different PCM heights

age capacity of the system. A similar trend was observed for the PV efficiency (Figure 14(b)), wherein a thickness of 4 mm generally maintained the highest efficiency, whereas an increased thickness of 6 mm gave the lowest efficiency. Since the PV efficiency is directly influenced by the operating temperature, superior thermal regulation leads to improved performance. Thus, an Al thickness of 4 mm provides the optimal balance between heat conduction and PCM heat storage under the investigated conditions.

A summary of the performance of all tested configurations and the selection of the optimal design is provided in Table S3 in the Supplementary Information.

Figure 15 presents a temperature contour comparison between the baseline PV panel and the optimized PV–PCM configuration during the peak heating and freezing stages of the orbital cycle. As expected, the baseline PV panel exhibited a significantly higher temperature distribution during the peak heating stage ($t = 2700$ s) owing to continuous solar heat absorption without thermal storage. By contrast, the PV–PCM configuration demonstrated substantially lower temperatures and smoother thermal gradients, indicating that the PCM absorbed a considerable portion of the thermal energy via its phase-change process. The Al structure also promoted heat dissipation between the PV and PCM domains, improving the overall thermal regulation of the system. During the freezing stage ($t = 5390$ s), the PCM configuration maintained a more stable temperature distribution than the baseline case. This was attributed to the gradual release of stored latent heat from the PCM, which moderated the cooling rate and reduced sudden temperature variations. These results confirm that PCM integration effectively improves the thermal stability of the PV panel under orbital thermal cycling. Similar trends were reported by Liu and Li [10], who revealed that PCM-based thermal management significantly reduced temperature fluctuations in nanosatellite PV systems.

4. CONCLUSIONS

This study investigated the thermal behavior of a PV panel in space and examined the use of PCMs for passive thermal control under orbital conditions. It was observed that in the absence of a PCM, the PV panel exhibited large temperature fluctuations during the orbital cycle. The Si layer temperature increased to ~72 °C during sunlight exposure and dropped to almost −2 °C during the eclipse period, potentially reducing the system reliability and thermal stability. The incorporation of a PCM significantly enhanced the thermal behavior of the PV panel by reducing the temperature fluctuation range from ~74 °C in the baseline case to ~12 °C in the optimized PV–PCM configuration. This improvement was mainly attributed to latent heat absorption and release during the phase-change process. Additionally, the PCM type had a clear influence on system performance. Among the tested

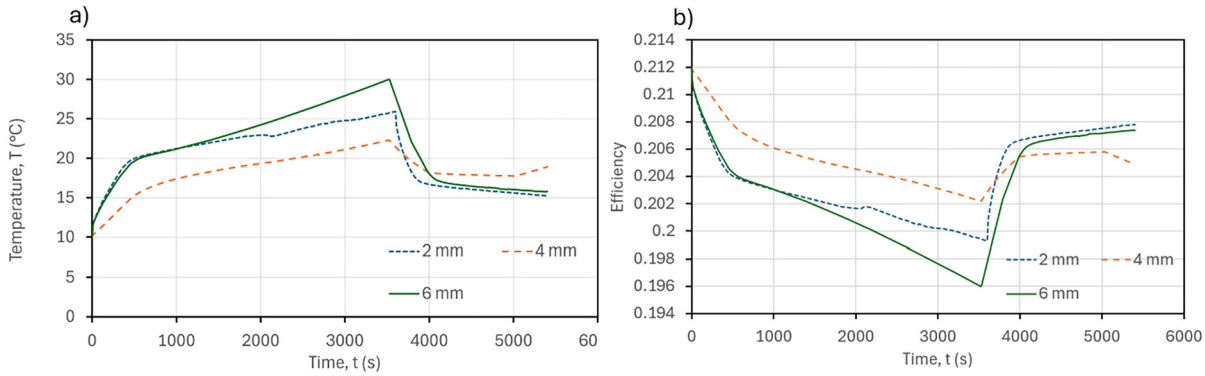


Figure 14. Effect of Al fin thickness on PV–PCM system performance: (a) Si layer temperature and (b) PV efficiency for Al thicknesses of 2, 4, and 6 mm, with corresponding PCM thicknesses of 48, 46, and 44 mm

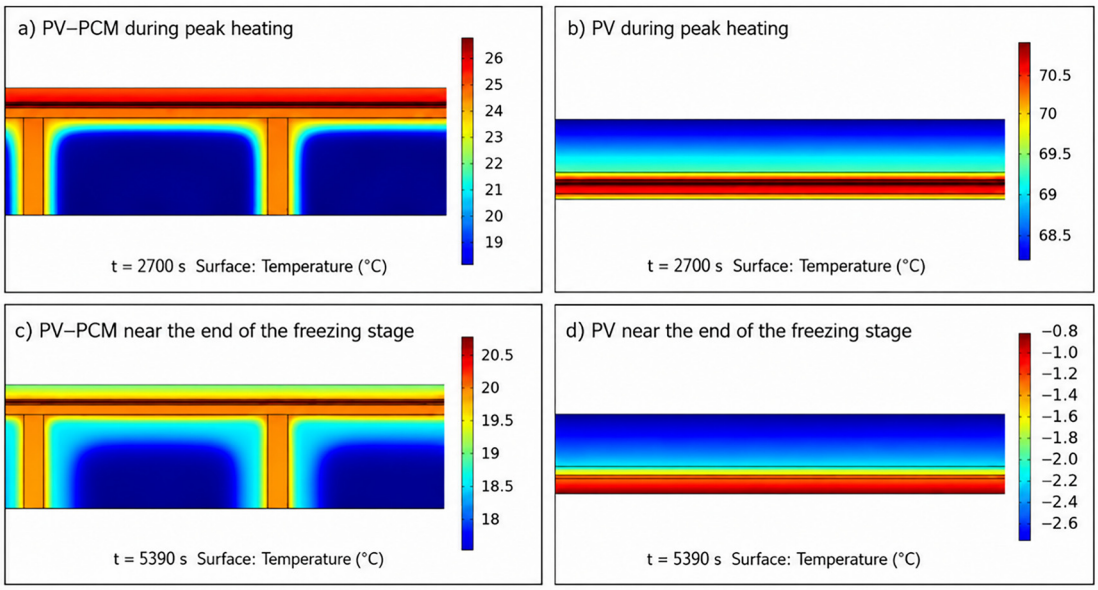


Figure 15. Temperature contour comparison between the baseline PV panel and the optimized PV–PCM configuration under orbital thermal cycling conditions: (a) PV–PCM during peak heating (t = 2700 s), (b) baseline PV panel during peak heating (t = 2700 s), (c) PV–PCM near the end of the freezing stage (t = 5390 s), and (d) baseline PV panel near the end of the freezing stage (t = 5390 s)

materials, n-hexadecane demonstrated superior thermal regulation performance, reducing the peak Si layer temperature from ~72 to ~22 °C, corresponding to a temperature reduction of ~69%. The superior performance of n-hexadecane is mainly due to its lower melting temperature, which enabled earlier activation of the phase-change process during heating. The Al fin thickness also influenced the thermal behavior of the system, with a thickness of 4 mm yielding superior performance (c.f., 2 and 6 mm) due to the optimal balance between heat conduction enhancement and effective PCM thermal storage. Furthermore, the PCM height had a noticeable effect on system performance. Specifically, the configuration with a height of 20 mm provided superior thermal regulation due to an effective balance between heat storage capacity and heat transfer. Increasing the PCM height beyond this value did not significantly improve system performance, as the low thermal conductivity of the PCM limited heat penetration into deeper PCM regions. Moreover, contour analysis demonstrated that PCM integration reduced localized temperature accumulation near the Si layer and produced smoother thermal gradients during both the heating and cooling stages of the orbital cycle, confirming the effectiveness of PCM-based passive thermal management under space conditions. Overall, these findings demonstrate that the integration of a PCM with an optimized Al structure can effectively regulate the temperature of space PV panels under orbital thermal cycling conditions. Future work should focus on the investigation of different fin geometries and evaluation of the effects of long-term thermal cycling on PCM performance and durability.

AFFILIATIONS AND AUTHOR DETAILS

Undergraduate Author

Ahmad Aloufi – *Department of Aerospace Engineering, King Fahd University of Petroleum & Minerals, Dhahran 31261, Saudi Arabia*; 0009-0003-2032-4758
Email: s202156790@kfupm.edu.sa

Corresponding Author

Naef A. A. Qasem – *Research Mentor, Professor, Department of Aerospace Engineering, King Fahd University of Petroleum & Minerals, Dhahran 31261, Saudi Arabia*; 0000-0002-3641-3996
Email: naefqasem@kfupm.edu.sa

ACKNOWLEDGEMENTS

The authors acknowledge the support provided by KFUPM through the Department of Aerospace Engineering and Deanship of Research under Project No. DUP2502.

REFERENCES

(1) Massachusetts Institute of Technology. Study: Climate change will reduce the number of satellites that can safely orbit in space. (2025).

(2) NASA Small Spacecraft Systems Virtual Institute. Power Subsystems. *NASA* (2025).

(3) Dubey, S., Sarvaiya, J. N. & Seshadri, B. Temperature dependent photovoltaic (PV) efficiency and its effect on PV production in the world - A review. in *Energy Procedia* vol. 33 311–321 (Elsevier Ltd, 2013).

(4) Peng, Z., Herfatmanesh, M. R. & Liu, Y. Cooled solar PV panels for output energy efficiency optimisation. *Energy Convers. Manag.* **150**, 949–955 (2017).

(5) Liu, T., Sun, Q., Meng, J., Pan, Z. & Tang, Y. Degradation modeling of satellite thermal control coatings in a low Earth orbit environment. *Solar Energy* **139**, 467–474 (2016).

(6) Sutheesh, P. M. & Chollackal, A. Thermal performance of multilayer insulation: A review. in *IOP Conference Series: Materials Science and Engineering* vol. 396 (Institute of Physics Publishing, 2018).

(7) NASA Small Spacecraft Systems Virtual Institute. Thermal Control. *NASA* (2025).

(8) Choi, M. K. *Paraffin Phase Change Material for Maintaining Temperature Stability of IceCube Type of CubeSats in LEO*. (2017).

(9) Hussain, B., Malik, H. W., Hasnain, F. U. & Irfan, M. Phase Change Material for the Cooling of Solar Panels—An Experimental Study †. *Engineering Proceedings* **45**, (2023).

(10) Liu, Q. Y. & Li, Y. Z. Thermal stability enhancement of fixed solar panels in nanosatellites based on phase change materials: a thermal-electrical coupling analysis. *Appl. Therm. Eng.* **284**, (2026).

(11) COMSOL AB. *Heat Transfer Module User's Guide, Version 6.3*. (2024).

(12) Dubey, S., Sarvaiya, J. N. & Seshadri, B. Temperature dependent photovoltaic (PV) efficiency and its effect on PV production in the world - A review. in *Energy Procedia* vol. 33 311–321 (Elsevier Ltd, 2013).

(13) Kopp, G. & Lean, J. L. A new, lower value of total solar irradiance: Evidence and climate significance. *Geophys. Res. Lett.* **38**, (2011).

(14) Riverola, A. *et al.* Mid-infrared emissivity of crystalline silicon solar cells. *Solar Energy Materials and Solar Cells* **174**, 607–615 (2018).

(15) Khyani, H. K., Vajpai, J., Karwa, R. & Bhadu, M. Thermal Modeling of Photovoltaic Panel for Cell Temperature and Power Output Predictions under Outdoor Climatic Conditions of Jodhpur. *Journal of Electrical and Computer Engineering* **2023**, (2023).

(16) Marzouk, S. A. *et al.* Thermal performance enhancement of phase change material melting using innovative fins. *Thermal Science and Engineering Progress* **61**, (2025).

(17) Bria, A. *et al.* Effect of PCM thickness on the performance of the finned PV/PCM system. in *Materials Today: Proceedings* vol. 72 3617–3625 (Elsevier Ltd, 2023).